Neuropharmacology 262 (2025) 110183

Contents lists available at ScienceDirect

Neuropharmacology

journal homepage: www.elsevier.com/locate/neuropharm

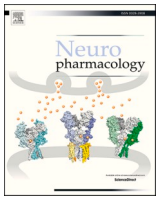

Glyphosate impairs both structure and function of GABAergic synapses in hippocampal neurons

Giuseppe Chiantia [a,1], Debora Comai [a,1], Enis Hidisoglu [b,c], Antonia Gurgone [a], Claudio Franchino [b], Valentina Carabelli [b], Andrea Marcantoni [b,**], Maurizio Giustetto [a,*]

[a] "Rita Levi-Montalcini" Department of Neuroscience, University of Turin, Turin, Italy
[b] Department of Drug Science, University of Turin, Turin, Italy
[c] Department of Biophysics, Faculty of Medicine, Izmir Bakircay University, Izmir, Turkey

ARTICLE INFO

Handling Editor: Dr M. Roberto

Keywords:
Glyphosate
GABAergic synapses
Hippocampal neurons
Patch-clamp
Immunocytochemistry
Gephyrin

ABSTRACT

Glyphosate (Gly) is a broad-spectrum herbicide responsible for the inhibition of the enzyme 5-enolpyruvylshikimate-3-phosphate synthase known to be expressed exclusively in plants and not in animals. For decades Gly has been thought to be ineffective in mammals, including humans, until it was demonstrated that rodents treated with the Gly-based herbicide Roundup showed reduced content of neurotransmitters (e.g., serotonin, dopamine, norepinephrine, and acetylcholine), increased oxidative stress in the brain associated with anxiety and depression-like behaviors and learning and memory deficits. Despite compelling evidence pointing to a neurotoxic effect of Gly, an in-depth functional description of its effects on synaptic transmission is still lacking. To investigate the synaptic alterations dependent on Gly administration we performed whole-cell patch-clamp recordings and immunocytochemistry on mouse primary cultured hippocampal neurons. Our findings reveal that 30 min incubation of Gly at the acceptable daily intake dose severely impaired inhibitory GABAergic synapses. Further analysis pointed out that Gly decreased the number of postsynaptic $GABA_A$ receptors and reduced the amplitude of evoked inhibitory postsynaptic currents, the readily releasable pool size available for synchronous release and the quantal size. Finally, a decreased number of release sites has been observed. Consistently, morphological analyses showed that the density of both pre- and post-synaptic inhibitory compartments decorating pyramidal cell dendrites was reduced by Gly. In conclusion, our experiments define for the first time the effects induced by Gly on GABAergic synapses, and reveal that Gly significantly impairs both pre- and post-synaptic mechanisms.

1. Introduction

Glyphosate (Gly), the active compound of the most used agriculture pesticides worldwide, blocks the shikimate pathway by inhibiting the enzyme 5-enolpyruvylshikimate-3-phosphate synthase (EPSPS). This latter is known to be expressed exclusively in plants, but not in mammals and other vertebrates. The shikimate pathway is a key metabolic system in plants that starts with phosphoenolpyruvate and erythrose 4-phosphate and proceeds to the biosynthesis of the aromatic amino acids phenylalanine, tyrosine, and tryptophan. Phosphoenolpyruvate and erythrose 4-phosphate undergo seven metabolic stages before synthesizing shikimate and chorismate, which serves as the starting point for the specific biosynthesis of aromatic amino acids (Shende et al., 2024). Gly mimics an intermediate state of the enzyme-substrates complex in the shikimate pathway, inhibiting the EPSPS, an important enzyme that catalyzes the conversion of shikimate-3-phosphate to 5-enolpyruvylshikimate-3-phosphate (Schönbrunn et al., 2001). In view of this property, Gly was considered essentially non-toxic for animals, humans included, until the presence of EPSPS has been found in human gut microbiota, where it plays a pivotal role in human physiology and pathology (Puigbo et al., 2022; Rueda-Ruzafa et al., 2019). Because Gly has been widely used over the last 40 years, residues of Gly and aminomethylphosphonic acid, its major bioactive metabolite, are now found at significant concentrations in foods containing wheat, soybeans, barley, and several

* Corresponding author. Università di Torino, Department of Neuroscience, C.so Raffaello 30, 10125, TORINO, Italy.
** Corresponding author. Università di Torino, Department of Drug Science, C.so Raffaello 30, 10125, TORINO, Italy.
E-mail addresses: andrea.marcantoni@unito.it (A. Marcantoni), maurizio.giustetto@unito.it (M. Giustetto).
[1] These authors contributed equally to this work.

https://doi.org/10.1016/j.neuropharm.2024.110183
Received 23 July 2024; Received in revised form 17 September 2024; Accepted 10 October 2024
Available online 12 October 2024

other crops (Bøhn et al., 2014). It has long been demonstrated that, after oral intake, Gly is rapidly absorbed, poorly metabolized, widely distributed in the body and does not reach the enterohepatic circulation (Bradberry et al., 2004). In addition, Gly oral bioavailability is generally low, ranging between 20 and 40% in humans and animal models, while dermal absorption remains even lower at less than 2% (Anadon et al., 2009; EFSA, 2015). However, Gly has been shown to accumulate in certain tissues, potentially leading to chronic toxic effects over time (Mesnage et al., 2015). Absorbed Gly has been shown to induce a low and acute toxicity while the non-absorbed portion is mostly eliminated through feces and urinary excretion (Faniband et al., 2021). Consistently, since 2015, Gly has been classified as a potentially carcinogenic substance (Guyton et al., 2015), while in 2017, the European Commission deliberated for an extension of the current maximum limit of exposure, setting as acceptable daily intake (ADI) the concentration of 0.5 mg/kg body weight (BW) per day (EFSA, 2017). Nevertheless, several association studies correlated Gly intoxication with neurological signs in humans, like parkinsonism, autism and Alzheimer's disease (Eriguchi et al., 2019; Pu et al., 2020). Furthermore, it has been observed that Gly exposure leads to cognitive dysfunction in rodents such as deficits in learning and memory (Ait Bali et al., 2019, 2022; Ait-Bali et al., 2020; Coullery et al., 2016), suggesting that the hippocampus, a region crucial for memory formation, is particularly vulnerable to the effect of Gly. In this regard, learning and memory consolidation depend on activity-dependent changes of both excitatory and inhibitory synapses (Kullmann and Lamsa, 2007), however the impact of Gly on the GABAergic system remains unexplored. So far, only one study conducted in *C. elegans* pointed out the possibility that Gly may have important effects on inhibitory transmission (Naraine et al., 2022). This lack of studies suggests that further investigations to fully understand the potential impact of Gly on inhibitory connectivity system are needed. Indeed, GABAergic neurotransmission plays a crucial role in governing cognitive functions (Tang et al., 2021). In this regard, 15–20% of central neurons are GABAergic interneurons (INs), while the majority (75–80%) are excitatory neurons (den Boon et al., 2015; Pelkey et al., 2017). Although the population of INs providing inhibitory input onto pyramidal neurons is relatively small, the delicate balance between excitation and inhibition (E/I) is consistently maintained at approximately 20% excitation and 80% inhibition (den Boon et al., 2015) reinforcing the idea that GABAergic INs play a pivotal role in mediating neuronal homeostasis by inducing hyperpolarization of the cell membrane. In this regard, INs serve as key regulators of cell excitability, effectively establishing the temporal pattern of synaptic excitation by orchestrating the precise timing of both input and output transmission (Pelkey et al., 2017) through mechanisms of spontaneous, synchronous and asynchronous neurotransmitter release (Kaeser and Regehr, 2014). Moreover, GABAergic inhibitory neurotransmission is essential in regulating brain rhythms and spontaneous neuronal activities throughout the developmental process (Zhao et al., 2021). Notably, E/I imbalance has been implicated in the underlying neurophysiological mechanisms of several neuropsychiatric disorders, such as schizophrenia, depression, anxiety and autism spectrum disorders (ASDs) (Amin et al., 2006; Mohler, 2012; Morello et al., 2018; Pizzo et al., 2016; Zhao et al., 2021). Because it has been shown that in rodents Gly can produce severe behavioural changes that stem from E/I imbalance, we explored whether the function of inhibitory synapses may be impaired by Gly (Costas-Ferreira et al., 2022). To this end, we examined inhibitory neurotransmission in primary cultured hippocampal neurons by using patch clamp recordings. Our results show that Gly impairs both pre- and postsynaptic GABAergic responses. Patch clamp experiments demonstrated that while Gly exposure increases the amount of asynchronous release, it decreases the spontaneous release by reducing both amplitude and frequency of miniature inhibitory postsynaptic currents (mIPSCs). Moreover, Gly altered the synchronous release by decreasing the average amplitude of evoked inhibitory postsynaptic currents (eIPSCs), an effect induced by the decreased number of postsynaptic GABAergic receptors of presynaptic release sites (N_{min}) together with the decreased size of the readily releasable pool available for synchronous release (RRP_{syn}). Finally, by using confocal microscopy analysis we show that the density of both pre- and post-synaptic inhibitory structures was reduced after Gly exposure. Taken together, our results indicate that GABAergic synapses of primary cultured hippocampal neurons are severely impaired by Gly administration.

2. Materials and methods

Ethical approval

Ethical approval was obtained for all experimental protocols from the University of Torino Animal Care and Use Committee, Torino, Italy. All experiments were conducted in accordance with the National Guide for the Care and Use of Laboratory Animals adopted by the Italian Ministry of Health (Authorization DGSAF 00 11710-P-26/07/2017). All animals had free access from the shelter to water and food. Every effort was made to minimize the number of animals used. Pregnant female mice were obtained in our laboratory where the mating occurred. For removal of embryos, animals were exposed to a rising concentration of CO_2, leading to loss of consciousness and were then rapidly sacrificed by cervical dislocation.

2.1. Cell preparation

Hippocampal neurons were obtained from 18-day-old embryo of C57BL/6 mice. The mice were sacrificed by inhalation of CO_2, and embryos were removed immediately by cesarean section. After dissection under sterile conditions, the hippocampi were kept in cold HBSS (4 °C) with high glucose, and then digested with papain (0.5 mg/mL), dissolved in HBSS plus DNAse (0.1 mg/mL) as previously described (Gavello et al., 2012). The isolated cells were then plated on round cover glasses (12 mm) for the immunofluorescence and on dishes (35 × 10 mm) with four inner rings for electrophysiological recordings, at the final density of 100 cells/mm^2, and were maintained in a culture medium consisting of Neurobasal, B-27 (1:50 v/v), glutamine (1% w/v), penicillin-streptomycin 1% (all from purchased by Sigma-Aldrich). Every 7 days for 2–3 weeks, a half-volume of the medium was replaced. To examine the effects of Gly on cultured neurons, after 18 days in vitro (DIV), cultures were treated with 0.5 μg/mL (3 μM) of Gly (Sigma-Aldrich, cat. 45521), in distilled water for 30 min. In control cultures, the same volume of distilled water was added for 30 min.

2.2. Electrophysiology

Patch-clamp electrodes, fabricated from thick borosilicate glasses (Hilgenberg, Mansifield, Germany), were pulled to a final resistance of 6–8 mΩ. Patch clamp recordings were performed in whole cell configuration using a Multiclamp 700-B amplifier connected to a Digidata 1440 and governed by the pClamp 10 software (Axon Instruments, Molecular Devices, Sunnyvale, CA, USA). Experiments were performed at room temperature (22–24 °C) in whole cell configuration and data were acquired with sample frequency of 10 kHz (Baldelli et al., 2007). Currents were filtered at half the acquisition rate with an eight-pole low-pass Bessel filter (1 kHz). Recordings with leak current > 100 pA or series resistance >20MΩ were discarded. Both mIPSCs and eIPSCs were recorded by holding neurons at −70 mV (V_h) (Gurgone et al., 2023). The amplitude and frequency of mIPSCs were calculated using a peak detector function with threshold amplitude set at 10 pA. Noise analysis of mIPSCs was performed with MiniAnalysis software (Synaptosoft, Decatur, GA, USA). Analysis of mIPSCs and eIPSCs amplitudes were performed with Clampfit software (Axon Instruments).

Paired-pulse depression (PPD). The eIPSCs associated with two consecutive pulses separated by interpulse intervals of increased duration (from 20 ms to 2 s), repeated every 10 s, were recorded in order to

study GABAergic PPD. The %PPD was calculated as: PPD = [(P1-P2)* 100]/P1, where P1 and P2 are respectively the amplitude of the first and second eIPSC.

Cumulative amplitude analysis. The readily releasable pool (RRP) size was measured considering the cumulative amplitude analysis (Schneggenburger et al., 1999). Briefly, a train stimulus protocol, with a frequency of 40 Hz and a duration of 2 s, was applied to the presynaptic neuron (Gonzalez et al., 2014). The evoked currents are characterized by an early depression during the first stage of the protocol, before reaching a steady-state phase that is characterized by an equilibrium between released and recycled vesicles. The linear regression to t = 0 of the steady-state phase was assessed as the best linear fit with the greatest number of data points starting from the last data point (Fig. 4b–f). The RRP size was determined by considering the intercept of the linear fit on the y-axis; p_{ves} was determined by dividing the first eIPSC amplitude by the size of RRP_{syn}.

Delayed asynchronous release. The delayed asynchronous release was measured by comparing the charge of 1 s duration following the high frequency (40 Hz) stimulation with the first 25 ms of eIPSC charge recorded 10 s before stimulating presynaptic neurons at high frequency (40 Hz) (Forte et al., 2020). The charge of spontaneous release measured 1 s before the train was subtracted from values of asynchronous.

Multiple probability fluctuation analysis. The quantal size (Q_{av}), the release probability of a synaptic vesicle released from a release site (p_{rav}), and the number of independent release sites (N_{min}) were measured by plotting the variance (σ^2) of eEPSCs amplitude in function of their amplitudes recorded in different release probability conditions (Clements and Silver, 2000). Q_{av}, p_{rav} and N_{min} are extrapolated by considering the parabolic relationship between σ^2 and mean post-synaptic current amplitude (I_{av}), where $\sigma^2 = AI_{av} - BI_{av}^2$ and $I_{av} = N_{min}$ p_{rav} Q_{av} (Reid and Clements, 1999; Silver et al., 1998). Considering that $N_{min} = 1/B$; $Q_{av} = A/(1 + CV_i^2)$; $p_{rav} = I_{av}$ (B/A) $(1 + CV_i^2)$. CV_i is the coefficient of variation of mIPSC amplitudes at an individual release site. Release probability was varied adding different concentrations of Cd^{2+} (2, 4 and 6 μM) and Ca^{2+} (2 and 5 mM) to the external solution. I_{av} and σ^2 were calculated over a stable epoch of 20 events.

2.3. Solutions and drugs

For the recordings of mIPSCs, Tyrode's Standard solution was used as extracellular solution containing (in mM): 2 $CaCl_2$, 130 NaCl, 1 $MgCl_2$, 10 HEPES, 4 KCl, 10 glucose, pH 7.4. D-(−)-2 amino-5-phosphonopentanoic acid (D-AP5; 50 μM), 6,7 Dinitroquinoxalone-2,3-Dione (DNQX, 20 μM, Sigma Aldrich), and CGP58845 (5 μM) (Tocris) were added to the external solution to block NMDA, non-NMDA, and $GABA_B$ receptors, respectively. Tetrodotoxin (TTX, 0.3 μM, Tocris) was added to block spontaneous action potentials generation. eIPSCs were recorded by perfusing postsynaptic neurons with Tyrode's Standart solution supplemented with 6,7-Dinitroquinoxalone-2,3-Dione (DNQX, 20 μM, Sigma-Aldrich), D-(−)-2- amino-5-phosphonopentanoic acid (D-AP5; 50 μM) and CGP58845 (5 μM) (Tocris) were used for blocking AMPA dependent synaptic currents, NMDA dependent activated currents and presynaptic $GABA_B$ receptors, respectively. The standard internal solution was (in mM): 20 Cs-MSO_3, 90 CsCl, 10 HEPES, 5 EGTA, 2 $MgCl_2$, 4 ATP (disodium salt), and 15 Phosphocreatine (pH 7.4). eIPSCs were recorded by adding QX-314 (N-(2,6-dimethylphenyl carbamoylmethyl) triethylammonium bromide, 10 mM, Tocris) into the internal solution to block postsynaptic Na^+ currents activated during eIPSCs. Neurons were constantly superfused through a gravity system constituted by a multibarreld pipette with a single outlet and five inlets.

2.4. Immunocytochemistry

Cultured hippocampal neurons were fixed with paraformaldehyde (4% in 0.1M phosphate buffer, PB, pH 7.4) for 10 min at room temperature (RT), washed three times for 5 min each with 0.01M PBS (pH 7.4), and kept in a blocking solution containing 10% normal donkey serum (NDS) and 0.5% Triton X-100 for 1 h. Subsequently, the cells were incubated overnight at RT with the primary antibody in a solution containing 3% NDS and 0.5% Triton X-100 as follows: mouse *anti*-gephyrin, 1:500 (Synaptic Systems, Göttingen, Germany, cat. 147 011), rabbit *anti*-vGAT 1:500 (Synaptic Systems, Göttingen, Germany, cat. 131-002) and chicken anti-MAP2A/B 1:1000 (Immunological Sciences, Rome, Italy, cat. AB-10417). Neurons were then rinsed in 0.01M PBS and incubated with a solution containing an appropriate fluorescence secondary antibody (1:1000, Jackson ImmunoResearch, West Grove, PA, USA) with 3% NDS, and 0.5% Triton X-100. After several rinses in PBS, the glass coverslips were mounted on microscope slides using an anti-fade aqueous mounting medium (Dako, Italy).

2.5. Image acquisition and analysis

Five Z-stack (0.5 μm steps) images (1024 x 1024 pixel resolution, 8-bit) were acquired with a confocal microscope (LSM 900; Zeiss) at 2x digital zoom using a 40× oil immersion objective (N.A. 1.30) and pinhole set at 1 Airy unit. The same values of laser intensity, digital gain and offset background were used for each image acquisition session. Images of secondary dendrites were acquired from at least 30 excitatory neurons, showing a pyramidal-shaped soma, randomly selected for each experimental condition and from two independent experiments. Average intensity projection images were reconstructed and exported in TIFF format for analysis using dedicated software (Fiji, version 1.34S; National Institutes of Health, public domain). Synaptic puncta area and density were automatically detected using a specific tool (i.e., analyze particles) available in the Fiji software. The colocalization of vGAT and gephyrin immunosignals was evaluated based on the determination of the Pearson's correlation coefficient (PCC) using the Fiji plug-in JaCoP (Angelini et al., 2022; Bolte and Cordelières, 2006). Fiji was used to modify the brightness and contrast display for image visualization purposes only.

2.6. Statistical analysis

The data are presented as mean ± SEM. The normality test was assessed through the D'Agostino Pearson's normality test. For datasets that passed the normality test, statistical analysis was conducted using GraphPad Prism software (La Jolla, CA, USA) with a Student's t-test. When two sample groups were not normally distributed, we used the non-parametric Mann-Whitney's *U* test or, when specified, the Kolmogorov-Smirnov test. The level of statistical significance is indicated by the p-value: $p \leq 0.05$ = *, $p \leq 0.01$ = **, $p \leq 0.001$ = ***, $p \leq 0.0001$ = ****. Degrees of freedom values (U and t) are included in the figure legends. Finally, all the datasets were analyzed by an operator blinded to treatment conditions.

3. Results

3.1. Glyphosate lowers the amplitude of GABAergic eIPSCs

The measure of evoked inhibitory postsynaptic currents (eIPSCs) (Fig. 1a) showed that Gly administration reduces the amplitude of inhibitory GABAergic neurotransmission. In particular, Gly decreased eIPSCs amplitude (Fig. 1b) from 1.54 ± 0.16 nA (n = 20 cells) to 0.68 ± 0.11 nA (n = 19 cells). The mean area underlying eIPSC was reduced as well from 134.79 ± 21.48 pC to 49.35 ± 9.12 pC (Fig. 1c). The time course of eIPSCs deactivation was fitted by a double exponential function with a fast (τ_{fast}) and a slow (τ_{slow}) time constant. We also observed that Gly did not modify the kinetic of eIPSCs deactivation (Fig. 1d and e). In particular, in control neurons τ_{fast} was 38.95 ± 5.22 ms and τ_{slow} was 98.26 ± 15.85 ms, while after Gly administration τ_{fast} was 37.87 ± 6.06 ms and τ_{slow} 97.77 ± 16.58 ms. Altogether, these data indicate that

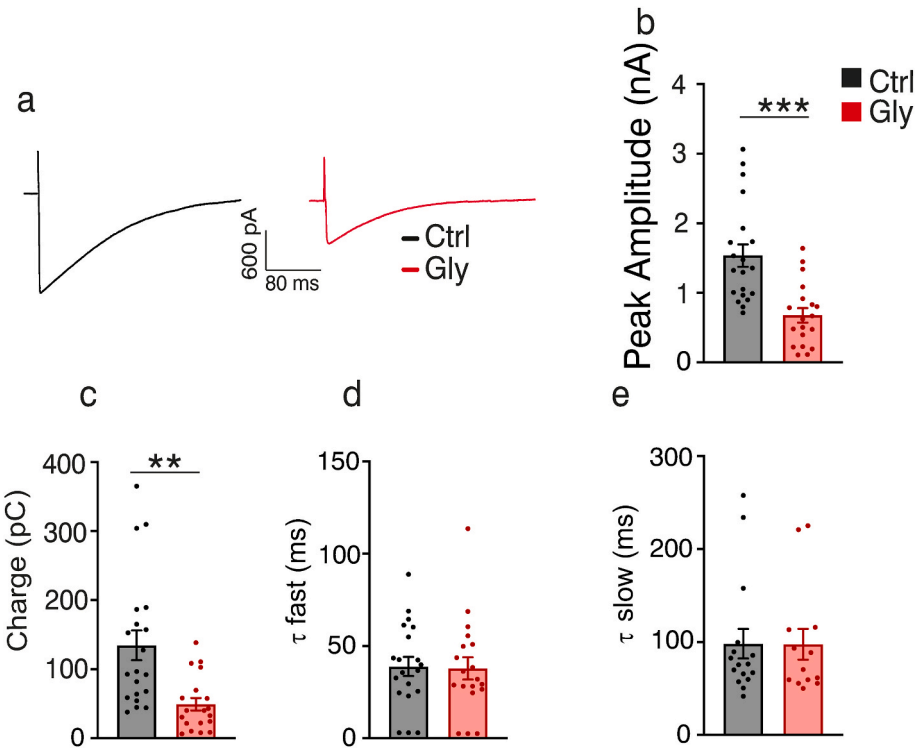

Fig. 1. Glyphosate decreases the amplitude of GABAergic eIPSCs, without affecting eEPSCs. (a) Representative traces of eIPSCs in control and after 30 min Gly exposure. (b) Bar graphs showing the mean amplitude of eIPSCs in control and after Gly (3 μM) treatment (t (4.27) = 31.74; ***p < 0.001, Student's t-test). (c) Bar graph representing the charge (pC) of eIPSCs (U (63); **p < 0.01, Mann-Whitney test). (d, e) Bar graph showing the time courses of eIPSCs deactivation, fitted with a slow and a fast time constant (τ_{slow} and τ_{fast}). (ctrl n = 20; Gly n = 19).

the decreased area of eIPSCs induced by Gly depends on the decreased eIPSCs amplitude and not by kinetic changes of $GABA_A$ receptors deactivation.

3.2. Glyphosate decreases GABAergic mIPSC amplitude and frequency

In order to assess the synaptic impairments responsible for eIPSCs reduction produced by Gly, we first focused on mIPSCs (Fig. 2a). Interestingly, we observed that Gly caused a significant decrease of mIPSCs amplitude (Fig. 2b) and an increase of the interevent interval (IEI) (Fig. 2c). In particular, the amplitude (Fig. 2b, inset) decreased on average from 46.35 ± 1.02 pA, (n = 11 cells, n = 444 events) to 39.76 ± 1.29 pA, (n = 14 cells, n = 211 events) after Gly-administration and the mean IEI (Fig. 2c, inset) increased from 306.30 ± 16.67 ms to 495.02 ± 41.77 ms. We next performed a peak-scaled variance analysis (PSVA) of mIPSCs in order to investigate whether Gly affected the number of postsynaptic $GABA_A$ receptors ($GABA_A$Rs) and their mean unitary current (*i*) (Hidisoglu et al., 2022; Russo et al., 2019). We used a parabolic fit to plot the distribution of mIPSCs variance (σ^2) as a function of their amplitude and measured the number of $GABA_A$Rs activated by a quantum of neurotransmitter (*N*) together with their unitary current (*i*). Intriguingly, we found that Gly decreased the width (*N*i*) of the parabolic fit (Fig. 2d and e) associated with a 60% reduction of the number of $GABA_A$Rs activated by *N* (Ctrl: 30.59 ± 9.28; Gly: 10.96 ± 1.27) (Fig. 2f). We also observed that Gly did not modify the initial steepness of the parabolic fit, that is associated to the unitary current (*i*) of a single $GABA_A$R (Traynelis and Jaramillo, 1998) (Ctrl *i:* 2.77 ± 0.31 pA; Gly *i*: 2.79 ± 0.26 pA) (Fig. 2g). These data indicate that Gly alters GABAergic synaptic transmission by targeting postsynaptic $GABA_A$ receptors and reducing their number rather than affecting their unitary current.

3.3. Glyphosate does not affect the short-term synaptic plasticity of GABAergic synapses

The increased IEI of mIPSCs induced by Gly suggests a possible presynaptic impairment of GABAergic transmission. To test this idea, we assessed whether Gly could affect GABA release probability (p) by measuring the PPD that follows the stimulation of a presynaptic inhibitory neuron with a paired protocol with increasing inter-pulse intervals (from 25 ms to 2 s) (Hidisoglu et al., 2022; Marcantoni et al., 2020) (Fig. 3a). In control neurons, the percentage of PPD versus IEI decreased following a double exponential decay with τ_{fast} = 2.77 ms and τ_{slow} = 162.34 ms (Fig. 3b) and PPD decreased from 81.38 ± 4.83 % to 12.28 ± 3.42 % when the IEI increased from 20 ms to 2 s (n = 8). Similar findings were observed after Gly treatment: PPD was 91.60 ± 2.44 % for IEI of 20 ms, while decreased to 15.98 ± 3.88 % for IEI of 2 s, indicating that p is not affected by Gly administration.

3.4. Glyphosate decreases the size of synchronous readily releasable pool at inhibitory synapses and increases the contribution of asynchronous GABA release

The presynaptic impairments induced by Gly were further investigated by stimulating INs for 2 s at 40 Hz to assess the dynamics of GABA release (Hidisoglu et al., 2022; Marcantoni et al., 2020). We observed that the peak amplitude of the evoked currents decreased over time, until reaching a steady-state condition both in control cultures and in the presence of Gly (Fig. 4a). This behavior reflects the equilibrium condition between vesicle release and vesicle replenishment reached at the steady state. The backward linear extrapolation of eIPSC cumulative amplitudes (Fig. 4b) furnishes an estimate of RRP_{syn}, evaluated as the intercept on the y-axis. Interestingly, our results show that RRP_{syn} is significantly reduced by Gly (Fig. 4c), from 3.72 ± 0.61 nA (n = 8) to 1.93 ± 0.49 nA (n = 8). Moreover, this decrease is not accompanied by a

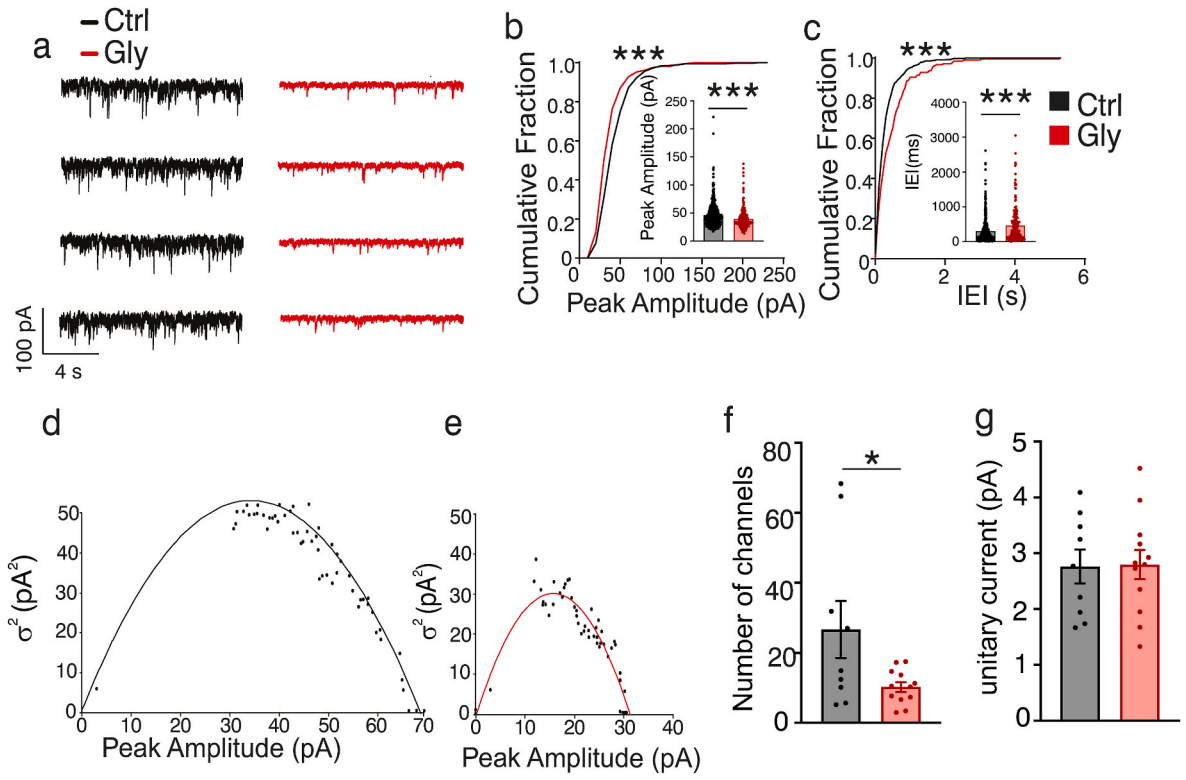

Fig. 2. Glyphosate reduces both amplitude and frequency of mIPSCs. (a) Representative mIPSCs recorded in hippocampal neurons in control condition and after 30 min treatment with Gly (3 μM). (b) Cumulative distribution of mIPSCs amplitude and (c) inter-event intervals (IEI) and relative bar graphs (insight), summarizing the average peak amplitude (D (0.22); ***$p < 0.001$, Kolmogorov-Smirnov test) and IEI (D (0.21); ***$p < 0.001$, Kolmogorov-Smirnov test). (d, e) Parabolic fit of mIPSCs variance (σ^2) in function of their amplitude in control and in the presence of Gly, respectively. (f) Bar graphs of the effects of Gly on the number of $GABA_A$ receptors activated by single quantum of neurotransmitter (t (2.29) = 19; *$p < 0.05$, Student's t-test) and on the average unitary current amplitude of $GABA_A$ receptors. (ctrl n = 14 cells, n = 444 events; Gly n = 11 cells, n = 211 events).

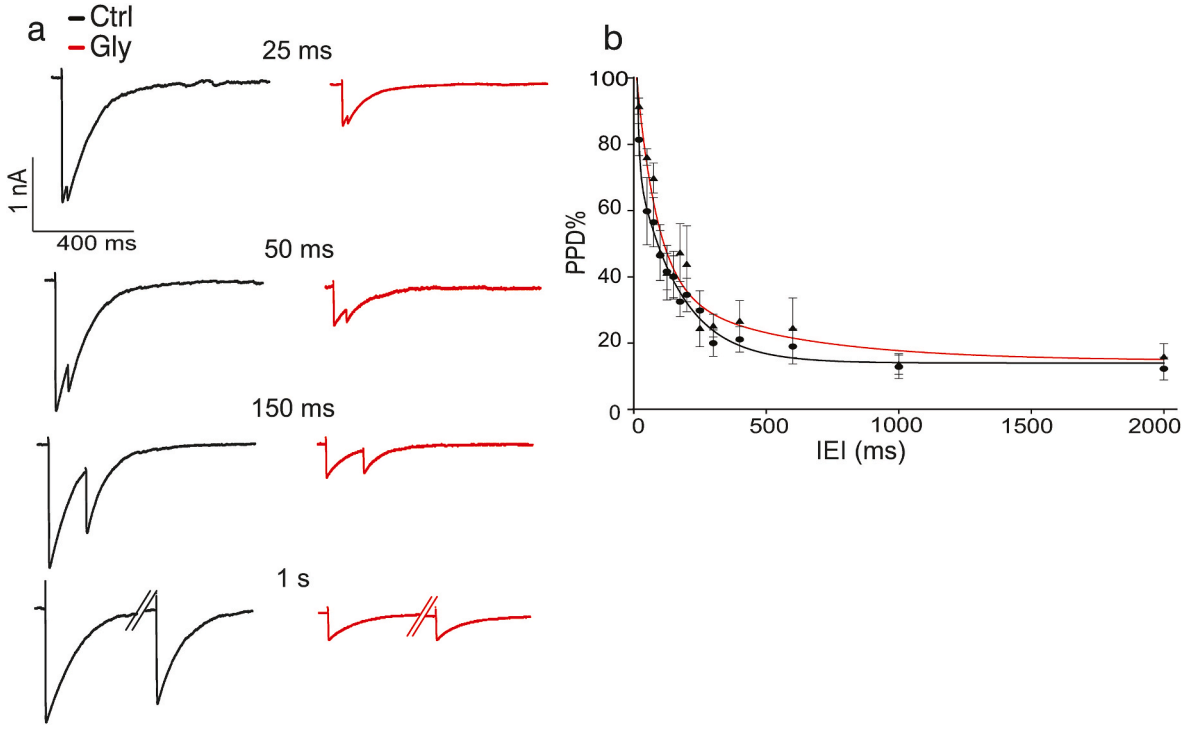

Fig. 3. Paired-pulse ratio is not altered by Glyphosate. (a) Traces representing PPD in control neurons and in the presence of Gly. (b) The percentage of PPD is plotted in function of inter-event intervals of pairs of stimuli without observing any significant effects induced by Gly. (ctrl n = 8; Gly n = 10 cells).

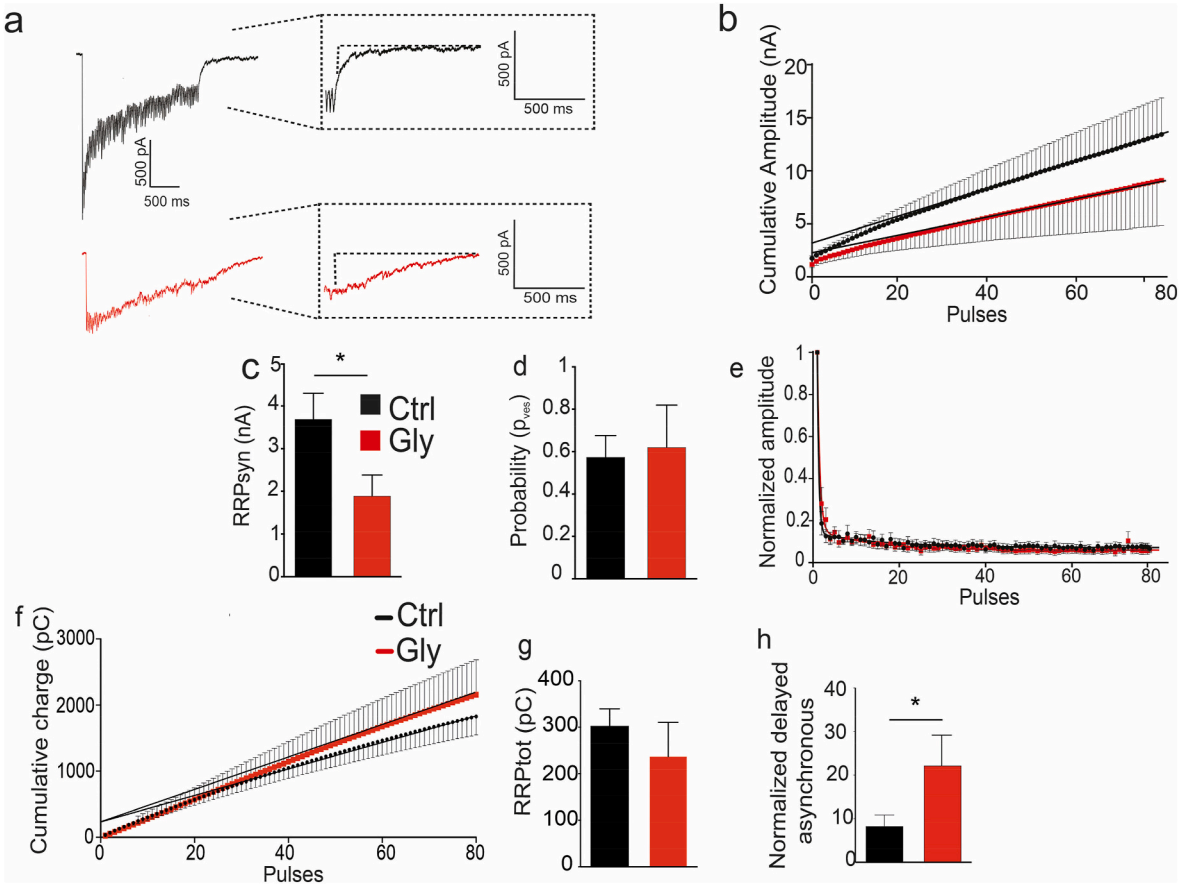

Fig. 4. Glyphosate affects neurotransmitter release.
(a) Representative traces of eIPSCs recorded during high frequency (40 Hz) stimulation for 2 s in ctrl (black trace) and in the presence of Gly (red trace). Insets represent the initial 1 s recording (dotted lines) after the end of the stimulation. (b) Cumulative eIPSCs amplitudes were measured in control condition and in the presence of Gly. The intercept of linear fits with y-axes gives an estimation of synchronous RRP_{syn} size. (c) Bar graph summarizing the effects of Gly on RRP_{syn} size ($t_{(2.31)} = 14$; *$p < 0.05$, Student's t-test) as well as on neurotransmitter release probability (d). (e) Time course of normalized eIPSCs in control and treated conditions indicates that the kinetic of release is not affected by Gly. (f) Cumulative eIPSC charge measured during 40 Hz stimulation for 2 s in ctrl and Glyphosate-treated neurons. (g) Bar graph representing the size of RRP_{tot}. (h) Bar graph comparing the amount of delayed asynchronous response normalized versus the synchronous release in ctrl and Gly ($U = 10$; *$p < 0.05$, Mann-Whitney test) (ctrl n = 8; Gly n = 8 cells). (For interpretation of the references to colour in this figure legend, the reader is referred to the web version of this article.)

reduction of the mean release probability (p_{ves}), defined as the probability that any given vesicle in the RRP_{syn} will be released (0.58 ± 0.10 in the control condition and 0.63 ± 0.20 in the presence of Gly treatment) (Fig. 4d). Finally, our results show that Gly did not alter the kinetic of deactivation of eIPSC amplitude during time (Fig. 4e). This latter was fitted by a double exponential curve with a fast τ_{fast} and a slow τ_{slow} time constant that were respectively 0.36 ms and 16.11 ms in control neurons and 0.57 ms and 13.33 ms in the presence of Gly.

We next assessed the cumulative curve of eIPSCs charge during 40 Hz stimulation, in order to study the size of the total readily release pool (RRP_{tot}) of vesicles available for synchronous and asynchronous release (Hidisoglu et al., 2022; Otsu et al., 2004) (Fig. 4f), without observing any significant effect induced by Gly administration. Indeed, RRP_{tot} was respectively 304.33 ± 40.99 pC (n = 8) in control condition and 239.40 ± 73.07 pC (n = 8) in Gly-treated neurons (Fig. 4g). Finally, by quantifying the charge of GABAergic current for 1 s following 40 Hz stimulation (Fig. 4a, insight), we compared the delayed asynchronous release versus the synchronous release (Hidisoglu et al., 2022; Medrihan et al., 2013). We found that while the delayed asynchronous release in control condition was 8.52 ± 2.58 times greater (n = 8) than the synchronous, this ratio increased to 22.43 ± 6.97 (n = 7) in the presence of Gly (Fig. 4h). Overall, these observations show that Gly interferes with GABA release without altering vesicle release probability, and that this effect is associated with the decreased size of the RRP_{syn}. Moreover, these data indicate that Gly produces a significant potentiation of the delayed asynchronous release from GABAergic synapses.

3.5. *Glyphosate decreases the number of GABAergic release sites without altering release probability*

We next performed the multiprobability fluctation analysis (MPFA) (Clements and Silver, 2000; Hidisoglu et al., 2022; Marcantoni et al., 2020) to assess the effect of Gly on GABAergic synaptic responses focusing on the average quantal size (Q_{av}), the number of independent release sites (N_{min}), and the average probability of a synaptic vesicle to be released from a release site (p_{rav}) (Clements and Silver, 2000). Different eIPSCs amplitudes were obtained by changing extracellular calcium or cadmium concentrations both in control condition (Fig. 5a) and in the presence of Gly (Fig. 5d). By plotting the variance (σ^2) of eIPSCs amplitudes (Fig. 5b–e) as a function of the average peak eIPSCs amplitude (I_{mean}), we obtained a parabolic distribution characterized by an initial steepness, a curvature and a size. These parameters were used for measuring Q_{av}, $p_{rav,}$ and $N_{min,}$ respectively (Fig. 5c–f). We observed that Gly decreased N_{min} (Ctrl: 165.90 ± 34.66; n = 12; Gly: 61.54 ± 8.37; n = 10) (Fig. 5g) and Q_{av} (Ctrl: 48.70 ± 7.57; n = 10; Gly: 19.24 ± 4.740; n = 10) (Fig. 5h), in agreement with the decreased number of GABAergic receptors (Fig. 2f). In contrast, p_{rav} remained unaltered (Ctrl: 0.57 ± 0.11; n = 12; Gly: 0.62 ± 0.12; n = 10) (Fig. 5i), in agreement

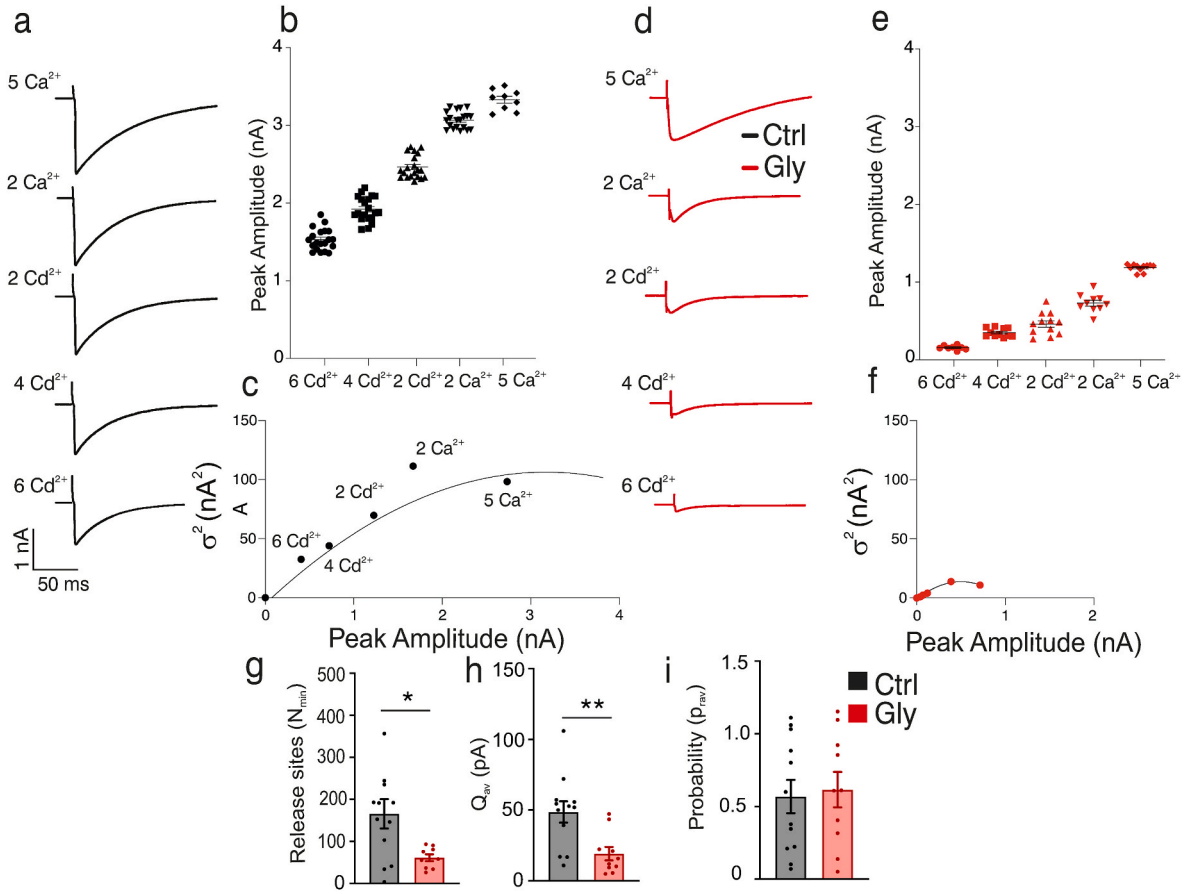

Fig. 5. Glyphosate decreases the number of release sites and quantal size. (a, d) Representative eIPSCs recorded in ctrl (a) and Gly-treated neurons (d) in different release probability conditions. (b, e) eIPSC amplitudes versus different extracellular Ca^{2+} and Cd^{2+} concentrations in ctrl and Gly-treated neurons. (c, f) Parabolic fit of the variance of eIPSC amplitude plotted versus the average amplitudes of eIPSCs. (g) Bar graph summarizing the estimated number of release sites of GABAergic synapses (t (2.93) = 12.26; *p < 0.05, Student's t-test); (h) the average quantal size (t (3.14) = 20; **p < 0.01, Student's t-test) and (I) the mean probability that a vesicle is released from the RRP_{syn}. (ctrl n = 12; Gly n = 10 cells).

with that observed previously on p and p_{ves} values. Taken together, these findings suggest that the decreased N_{min} induced by Gly contributes to a reduction in the amplitude of eIPSCs.

3.6. Both density and organization of GABAergic connections become atypical after glyphosate treatment

Finally, we assessed the structural organization of GABAergic synapses decorating the dendrites of hippocampal neurons after 30 min of either Gly or vehicle treatment. To this aim, we used double immunofluorescence with antibodies against the vesicular GABA transporter (vGAT), a presynaptic marker, and against gephyrin, the postsynaptic scaffolding protein of $GABA_A$ receptors (Pizzo et al., 2016) (Fig. 6a). Intriguingly, the quantitative analysis revealed that the exposure to Gly produced a 41% reduction of $vGAT^+$ puncta density (Ctrl: 3.17 ± 0.23, n = 29; Gly: 1.86 ± 0.17; n = 23; Fig. 6b), that was accompanied by a 28% decrease of $gephyrin^+$ puncta compared to vehicle (Ctrl: 3.88 ± 0.24, n = 31; Gly: 2.79 ± 0.18; n = 25; Fig. 6c). Moreover, while the size $vGAT^+$ puncta did not show any reduction after Gly treatment (Ctrl: 0.42 ± 0.03 μm^2, n = 25; Gly 0.41 ± 0.45 μm^2; n = 23; Fig. 6d), the size of $gephyrin^+$ puncta was significantly smaller after Gly (Ctrl: 0.26 ± 0.02 μm^2, n = 27; Gly: 0.20 ± 0.02 μm^2; n = 24; Fig. 1e). Finally, Gly treatment significantly decreased the density of vGAT-gephyrin synaptic appositions, as indicated by the Person's correlation coefficient (PCC) analysis (Ctrl: 0.53 ± 0.02, n = 33; Gly 0.4 ± 0.04; n = 29; Fig. 6f). These findings indicate that Gly is able to significantly alter GABAergic synaptic organization in hippocampal neurons by triggering the structural remodeling of inhibitory connections.

4. Discussion

The majority of risk assessment studies aiming at evaluating the safety of Gly-based herbicides were conducted more than 30 years ago and largely ignored the potential effects of Gly on the central nervous system. To address the safety of Gly, in this study we investigated the effects of this compound on both functional and structural organization of inhibitory synapses. Our findings provide insight into the precise mechanisms of action of Gly and demonstrate that an acute exposure (30 min) to 3 μM Gly, corresponding to the ADI concentration, reduces the number of GABAergic synaptic contacts, the rate of GABA release following neuronal excitation and the number of postsynaptic GABAergic receptors. In particular, we observed a robust decrease in the number of GABAergic synapses accompanied by their decreased functionality attributable to a presynaptic decrease of the number of release sites (N_{min}) and the size of RRP_{syn}, together with a postsynaptic decrease of the number of $GABA_A$ receptors. Moreover, we demonstrated that while the mechanisms governing spontaneous and synchronous release of GABA are inhibited by Gly, the asynchronous GABA release is potentiated, leaving open the question of the functional significance of this effect.

4.1. Methodological considerations

3 μM concentration used in this study corresponds to the ADI of Gly,

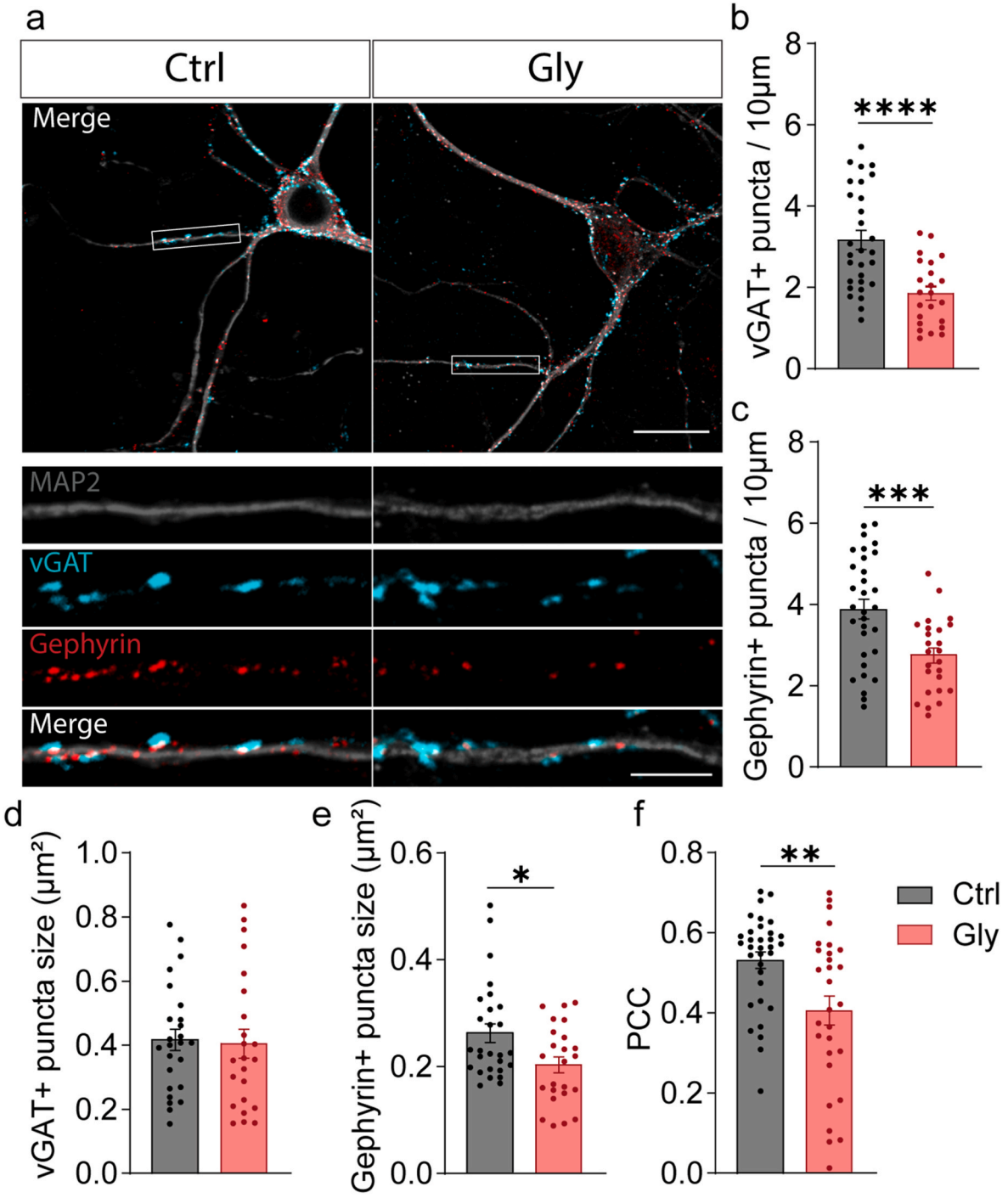

Fig. 6. Glyphosate alters both density and size of GABAergic synaptic contacts.
(a) Confocal microscopy images showing inhibitory synapses in control and Gly-exposed neurons. Scale bar: 20 µm. Inhibitory synapses were detected by using the presynaptic marker vGAT (cyan) and the postsynaptic marker gephyrin (red). The soma and dendrites were labelled with anti-MAP2 antibody. Boxed dendritic segments are shown as higher magnification images (below). Scale bar: 5 µm. (b, c) Bar graphs showing the average density of both vGAT ($t(4.33) = 50$; $^{****}p < 0.0001$, Student's t-test) and gephyrin ($t(3.39) = 54$; $^{***}p < 0.001$, Student's t-test) puncta. (d, e) Quantification of the averaged size of vGAT ($t(0.22) = 46$; $p > 0.05$, Student's t-test) and gephyrin puncta ($U = 211.5$; $^{*}p < 0.05$, Mann-Whitney test). (f) Quantification of the colocalization between vGAT with gephyrin immunosignals. PCC was calculated in dendrite-containing regions of interest ($U = 276$; $^{**}p < 0.01$, Mann-Whitney test). (For interpretation of the references to colour in this figure legend, the reader is referred to the web version of this article.)

which has been established through toxicological assessments and considered by European Food Safety Authority (EFSA) safe for chronic human exposure (EFSA, 2015). Our study aimed to investigate the physiological effects of Gly on GABAergic synapses, in order to generate data that are valuable for human risk assessments and relevant to regulatory evaluations for realistic exposure conditions. To this aim, we also considered that the NOEL (non-observed effect level) indicated by EFSA is two orders of magnitude higher than ADI (~200 µM). We compared these concentrations with the bioavailability of Gly (20%) and with the results obtained by Cattani et al. (2014) showing that 200 µM of Roundup, corresponding to 80 µM concentration of Gly, did not affect cell viability of hippocampal slices (Cattani et al., 2014). Finally,

we considered the manuscript of Arrigo et al. (2023) showing that μM concentrations of Gly are able to produce slight but significant modifications of cell viability and ROS production in H9c2 cell (Arrigo et al., 2023). As a result, we concluded that the concentration of 3 μM was suitable for studying whether in primary cultured hippocampal neurons Gly could be responsible for synaptic impairment without affecting cell survival. Moreover, we incubated neurons for 30 min with Gly before assessing its effect on inhibitory synapses following the previous study of Cattani et al. (2014) where a similar incubation time on rat hippocampal slices showed that Gly-based herbicide induces glutamatergic excitotoxicity and oxidative damage in neuronal cells (Cattani et al., 2014). Moreover, it has been shown that at low doses (1 μM–1 mM) Gly was able to significantly affect cell viability and increase oxidative stress in H9c2 cells after an incubation time of at least 1–2 h (Arrigo et al., 2023).

4.2. Gly inhibits the spontaneous release of GABA

Chemical synapses release neurotransmitters by alternative mechanisms (Kaeser and Regehr, 2014) each of those are considered important for specific neuronal functions. We first focused on spontaneous GABA release from hippocampal INs known to be involved in neurodevelopment and synapse maturation (Andreae et al., 2012; Ganguly et al., 2001). We noticed (Fig. 2) that Gly reduces both the amplitude and the frequency of mIPSCs and suggested that both pre- and postsynaptic sites of GABAergic synapses are affected by Gly. Importantly, these results are in agreement with our anatomical data (Fig. 6) showing that both the density and the organization of GABAergic contacts are severely altered by Gly exposure, strongly arguing that the decreased spontaneous release of GABA reflects a reduction of the total number of inhibitory synaptic contacts. In line with these conclusions, we suggest that the reduced mIPSCs amplitude induced by Gly is a direct consequence of the decreased number of $GABA_A$ receptors, whereas the reduced mIPSCs frequency is determined by the decreased RRP_{syn} size and N_{min} rather than by changes of vesicles release probability (Figs. 2–4). As a result, the effects of Gly on hippocampal GABAergic synapses could contribute to impair long-term synaptic plasticity and memory formation (Ait Bali et al., 2019) by altering neuronal network excitability. Moreover, Gly-induced alterations of GABA-mediated synaptic signaling could also contribute to the onset of different neurological disorders, including ASDs and neurodegenerative diseases (Forte et al., 2020). The hippocampus contains a variety of GABAergic INs, with a predominance of cholecystokinin$^+$ and parvalbumin$^+$ INs, which are distinguished for different GABA release mechanisms and involvement in a range of neuronal functions (Liu et al., 2006). In this perspective, future research should aim to determine whether Gly is accountable for distinct effects based on the different INs subtypes. Finally, it should be taken into account that here the effect of Gly has been investigated after 30 min since its application, therefore we cannot exclude that longer incubation time could be responsible for additional or different impairments.

4.3. Gly inhibits synchronous release of GABA

We have shown that Gly administration significantly decreases the amplitude of eIPSCs (Fig. 1) without affecting their kinetic decay (Fig. 1d and e). These findings, together with the absence of significant effects of Gly on $GABA_A$ receptors unitary current (Fig. 2g), strongly support the idea that the postsynaptic effect we observed depends on the reduction of the number of $GABA_A$ receptors rather than on changes of their subunit composition. Synchronous release of GABA is driven by action potential propagation at the presynaptic membrane that is responsible for the fast influx of Ca^{2+} through presynaptic voltage gated Ca^{2+} channels (Medrihan et al., 2013). Interestingly, at presynaptic sites the inhibitory effects of eIPSC amplitude induced by Gly nicely correlate with decreased RRP_{syn} size (Fig. 4c) and number of release sites (N_{min}) (Fig. 5g), while the decreased Q_{av} (Fig. 5h) is in agreement with the decreased number of $GABA_A$ receptors (Fig. 2f). Finally, because no changes of GABA release probability (p, p_{rav}) (Figs. 4 and 5) have been observed, our data suggest that the Ca^{2+-}dependent mechanisms responsible for synchronous release of GABA are likely not impaired by Gly.

4.4. Gly potentiates asynchronous release of GABA

Asynchronous GABA release increases during prolonged high-frequency synaptic stimulation and is important for preventing network hyperexcitability (Kaeser and Regehr, 2014). Recent reports revealed that asynchronous release is impaired in brain diseases such as epilepsy (Forte et al., 2020) and neurodegeneration (Chiantia et al., 2023). Compared to synchronous release, vesicles released asynchronously have higher sensitivity to calcium that accumulates at presynaptic site during prolonged stimulation and their release is impaired when intracellular calcium concentration is dysregulated, a process that occurs for example during the onset of Alzheimer's disease (Chiantia et al., 2023; Hidisoglu et al., 2022). Interestingly, our data reveal that while RRP_{syn} size is decreased by Gly, the size of RRP_{tot} remains unchanged (Fig. 4g), a result in agreement with our analysis on the size of $vGAT^+$ presynaptic terminals showing that Gly does not produce significant differences. These results indicate that Gly may increase the size of the pool of vesicles responsible for asynchronous release while it can decrease the pool of vesicles available for synchronous release.

In summary, in the present manuscript we investigated the effects of Gly on hippocampal neurons and observed an overall impairment of GABAergic synaptic structure and function. In particular, we demonstrated a decreased number of GABAergic synaptic contacts accompanied by a functional inhibition of GABAergic synapse attributable to a presynaptic decrease of the number of release sites (N_{min}) and the size of RRP_{syn} together with a postsynaptic decrease of the number of $GABA_A$ receptors. In addition, our findings show that while Gly selectively inhibits spontaneous and synchronous GABA release it enhances asynchronous GABA release, an interesting effect that will need further investigation to understand its functional relevance. Finally, the current dataset was collected using hippocampal neurons at 18 DIV developmental stage, when the reconstituted neuronal network is thought to be fully mature in terms of synaptic properties (Allio et al., 2015; Gavello et al., 2018). Because the effects of Gly during neurodevelopment are mostly unknown, it will be important in the future to assess synaptic connectivity by treating neurons with Gly at earlier *in-vitro* developmental stages.

CRediT authorship contribution statement

Giuseppe Chiantia: Writing – review & editing, Writing – original draft, Methodology, Investigation, Formal analysis, Data curation, Conceptualization. **Debora Comai:** Writing – review & editing, Methodology, Investigation, Formal analysis, Data curation, Conceptualization. **Enis Hidisoglu:** Writing – review & editing, Supervision, Methodology. **Antonia Gurgone:** Supervision, Methodology, Data curation. **Claudio Franchino:** Methodology, Investigation. **Valentina Carabelli:** Writing – review & editing, Supervision, Data curation. **Andrea Marcantoni:** Writing – review & editing, Writing – original draft, Supervision, Funding acquisition, Formal analysis, Data curation, Conceptualization. **Maurizio Giustetto:** Writing – review & editing, Writing – original draft, Supervision, Methodology, Funding acquisition, Formal analysis, Data curation, Conceptualization.

Funding

This work was supported by the following project: PRIN PNRR MUR 2022 (Prot. P2022CRAXJ) to AM, Progetto Trapezio (cod. 68002) funded by Compagnia San Paolo to VC; PRIN MUR 2022 (2022ARRYK8) to EH; Intesa San Paolo (B/2018/0058) and to MG. DC was supported by a

PhD scholarship from the FSE REACT-EU Program.

Declaration of competing interest

The authors declare that they have no competing financial or personal interests that could have appeared to influence the work reported in this paper.

Data availability

Data will be made available on request.

References

Ait Bali, Y., Kaikai, N.E., Ba-M'hamed, S., Bennis, M., 2019. Learning and memory impairments associated to acetylcholinesterase inhibition and oxidative stress following glyphosate based-herbicide exposure in mice. Toxicology 415, 18–25. https://doi.org/10.1016/j.tox.2019.01.010.

Ait Bali, Y., Kaikai, N.E., Ba-M'hamed, S., Sassoe-Pognetto, M., Giustetto, M., Bennis, M., 2022. Anxiety and gene expression enhancement in mice exposed to glyphosate-based herbicide. Toxics 10. https://doi.org/10.3390/toxics10050226.

Ait-Bali, Y., Ba-M'hamed, S., Gambarotta, G., Sassoè-Pognetto, M., Giustetto, M., Bennis, M., 2020. Pre- and postnatal exposure to glyphosate-based herbicide causes behavioral and cognitive impairments in adult mice: evidence of cortical ad hippocampal dysfunction. Arch. Toxicol. 94, 1703–1723. https://doi.org/10.1007/s00204-020-02677-7.

Allio, A., Calorio, C., Franchino, C., Gavello, D., Carbone, E., Marcantoni, A., 2015. Bud extracts from Tilia tomentosa Moench inhibit hippocampal neuronal firing through GABAA and benzodiazepine receptors activation. J. Ethnopharmacol. 172, 288–296. https://doi.org/10.1016/j.jep.2015.06.016.

Amin, Z., Mason, G.F., Cavus, I., Krystal, J.H., Rothman, D.L., Epperson, C.N., 2006. The interaction of neuroactive steroids and GABA in the development of neuropsychiatric disorders in women. Pharmacol. Biochem. Behav. 84, 635–643. https://doi.org/10.1016/j.pbb.2006.06.007.

Anadon, A., Martinez-Larranaga, M.R., Martinez, M.A., Castellano, V.J., Martinez, M., Martin, M.T., Nozal, M.J., Bernal, J.L., 2009. Toxicokinetics of glyphosate and its metabolite aminomethyl phosphonic acid in rats. Toxicol. Lett. 190, 91–95. https://doi.org/10.1016/j.toxlet.2009.07.008.

Andreae, L.C., Fredj, N.B., Burrone, J., 2012. Independent vesicle pools underlie different modes of release during neuronal development. J. Neurosci. 32, 1867–1874. https://doi.org/10.1523/JNEUROSCI.5181-11.2012.

Angelini, C., Morellato, A., Alfieri, A., Pavinato, L., Cravero, T., Bianciotto, O.T., Salemme, V., Natalini, D., Centonze, G., Raspanti, A., Garofalo, T., Valdembri, D., Serini, G., Marcantoni, A., Becchetti, A., Giustetto, M., Turco, E., Defilippi, P., 2022. p140Cap regulates the composition and localization of the NMDAR complex in synaptic lipid rafts. J. Neurosci. 42, 7183–7200. https://doi.org/10.1523/JNEUROSCI.1775-21.2022.

Arrigo, E., Gilardi, S., Muratori, L., Raimondo, S., Mancardi, D., 2023. Biological effects of sub-lethal doses of glyphosate and AMPA on cardiac myoblasts. Front. Physiol. 14, 1165868. https://doi.org/10.3389/fphys.2023.1165868.

Baldelli, P., Fassio, A., Valtorta, F., Benfenati, F., 2007. Lack of synapsin I reduces the readily releasable pool of synaptic vesicles at central inhibitory synapses. J. Neurosci. 27, 13520–13531. https://doi.org/10.1523/JNEUROSCI.3151-07.2007.

Bøhn, T., Cuhra, M., Traavik, T., Sanden, M., Fagan, J., Primicerio, R., 2014. Compositional differences in soybeans on the market: glyphosate accumulates in Roundup Ready GM soybeans. Food Chem. 153, 207–215. https://doi.org/10.1016/j.foodchem.2013.12.054.

Bolte, S., Cordelières, F.P., 2006. A guided tour into subcellular colocalization analysis in light microscopy. J. Microsc. 224, 213–232. https://doi.org/10.1111/j.1365-2818.2006.01706.x.

Bradberry, S.M., Proudfoot, A.T., Vale, J.A., 2004. Glyphosate poisoning. Toxicol. Rev. 23, 159–167. https://doi.org/10.2165/00139709-200423030-00003.

Cattani, D., de Liz Oliveira Cavalli, V.L., Heinz Rieg, C.E., Domingues, J.T., Dal-Cim, T., Tasca, C.I., Mena Barreto Silva, F.R., Zamoner, A., 2014. Mechanisms underlying the neurotoxicity induced by glyphosate-based herbicide in immature rat hippocampus: involvement of glutamate excitotoxicity. Toxicology 320, 34–45. https://doi.org/10.1016/j.tox.2014.03.001.

Chiantia, G., Hidisoglu, E., Marcantoni, A., 2023. The role of ryanodine receptors in regulating neuronal activity and its connection to the development of alzheimer's disease. Cells 12. https://doi.org/10.3390/cells12091236.

Clements, J.D., Silver, R.A., 2000. Unveiling synaptic plasticity: a new graphical and analytical approach. Trends Neurosci. 23, 105–113. https://doi.org/10.1016/s0166-2236(99)01520-9.

Costas-Ferreira, C., Durán, R., Faro, L.R.F., 2022. Toxic effects of glyphosate on the nervous system: a systematic review. Int. J. Mol. Sci. 23. https://doi.org/10.3390/ijms23094605.

Coullery, R.P., Ferrari, M.E., Rosso, S.B., 2016. Neuronal development and axon growth are altered by glyphosate through a WNT non-canonical signaling pathway. Neurotoxicology 52, 150–161. https://doi.org/10.1016/j.neuro.2015.12.004.

den Boon, F.S., Werkman, T.R., Schaafsma-Zhao, Q., Houthuijs, K., Vitalis, T., Kruse, C. G., Wadman, W.J., Chameau, P., 2015. Activation of type-1 cannabinoid receptor shifts the balance between excitation and inhibition towards excitation in layer II/III pyramidal neurons of the rat prelimbic cortex. Pflueg. Arch. Eur. J. Physiol. 467, 1551–1564. https://doi.org/10.1007/s00424-014-1586-z.

Efsa, E.F.S.A., 2015. Conclusion on the peer review of the pesticide risk assessment of the active substance glyphosate. EFSA J. 13 (4302). https://doi.org/10.2903/j.efsa.2015.4302.

Efsa, E.F.S.A., 2017. Peer review of the pesticide risk assessment of the potential endocrine disrupting properties of glyphosate. EFSA J. 15, e04979. https://doi.org/10.2903/j.efsa.2017.4979.

Eriguchi, M., Iida, K., Ikeda, S., Osoegawa, M., Nishioka, K., Hattori, N., Nagayama, H., Hara, H., 2019. Parkinsonism relating to intoxication with glyphosate. Intern. Med. 58, 1935–1938. https://doi.org/10.2169/internalmedicine.2028-18.

Faniband, M.H., Noren, E., Littorin, M., Lindh, C.H., 2021. Human experimental exposure to glyphosate and biomonitoring of young Swedish adults. Int. J. Hyg Environ. Health 231, 113657. https://doi.org/10.1016/j.ijheh.2020.113657.

Forte, N., Binda, F., Contestabile, A., Benfenati, F., Baldelli, P., 2020. Synapsin I synchronizes GABA release in distinct interneuron subpopulations. Cerebr. Cortex 30, 1393–1406. https://doi.org/10.1093/cercor/bhz174.

Ganguly, K., Schinder, A.F., Wong, S.T., Poo, M., 2001. GABA itself promotes the developmental switch of neuronal GABAergic responses from excitation to inhibition. Cell 105, 521–532. https://doi.org/10.1016/s0092-8674(01)00341-5.

Gavello, D., Calorio, C., Franchino, C., Cesano, F., Carabelli, V., Carbone, E., Marcantoni, A., 2018. Early alterations of hippocampal neuronal firing induced by Abeta42. Cerebr. Cortex 28, 433–446. https://doi.org/10.1093/cercor/bhw377.

Gavello, D., Rojo-Ruiz, J., Marcantoni, A., Franchino, C., Carbone, E., Carabelli, V., 2012. Leptin counteracts the hypoxia-induced inhibition of spontaneously firing hippocampal neurons: a microelectrode array study. PLoS One 7, e41530. https://doi.org/10.1371/journal.pone.0041530.

Gonzalez, J.C., Lignani, G., Maroto, M., Baldelli, P., Hernandez-Guijo, J.M., 2014. Presynaptic muscarinic receptors reduce synaptic depression and facilitate its recovery at hippocampal GABAergic synapses. Cerebr. Cortex 24, 1818–1831. https://doi.org/10.1093/cercor/bht032.

Gurgone, A., Pizzo, R., Raspanti, A., Chiantia, G., Devi, S., Comai, D., Morello, N., Pilotto, F., Gnavi, S., Lupori, L., Mazziotti, R., Sagona, G., Putignano, E., Nocentini, A., Supuran, C.T., Marcantoni, A., Pizzorusso, T., Giustetto, M., 2023. mGluR 5 PAMs rescue cortical and behavioural defects in a mouse model of CDKL5 deficiency disorder. Neuropsychopharmacology 48, 877–886. https://doi.org/10.1038/s41386-022-01412-3.

Guyton, K.Z., Loomis, D., Grosse, Y., El Ghissassi, F., Benbrahim-Tallaa, L., Guha, N., Scoccianti, C., Mattock, H., Straif, K., International Agency for Research on Cancer Monograph Working Group, I.L.F., 2015. Carcinogenicity of tetrachlorvinphos, parathion, malathion, diazinon, and glyphosate. Lancet Oncol. 16, 490–491. https://doi.org/10.1016/S1470-2045(15)70134-8.

Hidisoglu, E., Chiantia, G., Franchino, C., Tomagra, G., Giustetto, M., Carbone, E., Carabelli, V., Marcantoni, A., 2022. The ryanodine receptor-calstabin interaction stabilizer S107 protects hippocampal neurons from GABAergic synaptic alterations induced by Abeta42 oligomers. J. Physiol. 600, 5295–5309. https://doi.org/10.1113/JP283537.

Kaeser, P.S., Regehr, W.G., 2014. Molecular mechanisms for synchronous, asynchronous, and spontaneous neurotransmitter release. Annu. Rev. Physiol. 76, 333–363. https://doi.org/10.1146/annurev-physiol-021113-170338.

Kullmann, D.M., Lamsa, K.P., 2007. Long-term synaptic plasticity in hippocampal interneurons. Nat. Rev. Neurosci. 8 (9), 687–699. https://doi.org/10.1038/nrn2207.

Liu, Z., Neff, R.A., Berg, D.K., 2006. Sequential interplay of nicotinic and GABAergic signaling guides neuronal development. Science 314, 1610–1613. https://doi.org/10.1126/science.1134246.

Marcantoni, A., Cerullo, M.S., Buxeda, P., Tomagra, G., Giustetto, M., Chiantia, G., Carabelli, V., Carbone, E., 2020. Amyloid Beta 42 oligomers up-regulate the excitatory synapses by potentiating presynaptic release while impairing postsynaptic NMDA receptors. J. Physiol. 598, 2183–2197. https://doi.org/10.1113/JP279345.

Medrihan, L., Cesca, F., Raimondi, A., Lignani, G., Baldelli, P., Benfenati, F., 2013. Synapsin II desynchronizes neurotransmitter release at inhibitory synapses by interacting with presynaptic calcium channels. Nat. Commun. 4, 1512. https://doi.org/10.1038/ncomms2515.

Mesnage, R., Defarge, N., Spiroux de Vendomois, J., Seralini, G.E., 2015. Potential toxic effects of glyphosate and its commercial formulations below regulatory limits. Food Chem. Toxicol. 84, 133–153. https://doi.org/10.1016/j.fct.2015.08.012.

Mohler, H., 2012. The GABA system in anxiety and depression and its therapeutic potential. Neuropharmacology 62, 42–53. https://doi.org/10.1016/j.neuropharm.2011.08.040.

Morello, N., Schina, R., Pilotto, F., Phillips, M., Melani, R., Plicato, O., Pizzorusso, T., Pozzo-Miller, L., Giustetto, M., 2018. Loss of Mecp2 causes atypical synaptic and molecular plasticity of parvalbumin-expressing interneurons reflecting rett syndrome-like sensorimotor defects. eNeuro 5. https://doi.org/10.1523/ENEURO.0086-18.2018.

Naraine, A.S., Aker, R., Sweeney, I., Kalvey, M., Surtel, A., Shanbhag, V., Dawson-Scully, K., 2022. Roundup and glyphosate's impact on GABA to elicit extended proconvulsant behavior in Caenorhabditis elegans. Sci. Rep. 12, 13655. https://doi.org/10.1038/s41598-022-17537-w.

Otsu, Y., Shahrezaei, V., Li, B., Raymond, L.A., Delaney, K.R., Murphy, T.H., 2004. Competition between phasic and asynchronous release for recovered synaptic vesicles at developing hippocampal autaptic synapses. J. Neurosci. 24, 420–433. https://doi.org/10.1523/JNEUROSCI.4452-03.2004.

Pelkey, K.A., Chittajallu, R., Craig, M.T., Tricoire, L., Wester, J.C., McBain, C.J., 2017. Hippocampal GABAergic inhibitory interneurons. Physiol. Rev. 97, 1619–1747. https://doi.org/10.1152/physrev.00007.2017.

Pizzo, R., Gurgone, A., Castroflorio, E., Amendola, E., Gross, C., Sassoè-Pognetto, M., Giustetto, M., 2016. Lack of Cdkl5 disrupts the organization of excitatory and inhibitory synapses and parvalbumin interneurons in the primary visual cortex. Front. Cell. Neurosci. 10, 261. https://doi.org/10.3389/fncel.2016.00261.

Pu, Y., Yang, J., Chang, L., Qu, Y., Wang, S., Zhang, K., Xiong, Z., Zhang, J., Tan, Y., Wang, X., Fujita, Y., Ishima, T., Wang, D., Hwang, S.H., Hammock, B.D., Hashimoto, K., 2020. Maternal glyphosate exposure causes autism-like behaviors in offspring through increased expression of soluble epoxide hydrolase. Proc. Natl. Acad. Sci. U. S. A. 117, 11753–11759. https://doi.org/10.1073/pnas.1922287117.

Puigbo, P., Leino, L.I., Rainio, M.J., Saikkonen, K., Saloniemi, I., Helander, M., 2022. Does Glyphosate Affect the Human Microbiota? Life, Basel, p. 12. https://doi.org/10.3390/life12050707.

Reid, C.A., Clements, J.D., 1999. Postsynaptic expression of long-term potentiation in the rat dentate gyrus demonstrated by variance-mean analysis. J. Physiol. 518, 121–130. https://doi.org/10.1111/j.1469-7793.1999.0121r.x.

Rueda-Ruzafa, L., Cruz, F., Roman, P., Cardona, D., 2019. Gut microbiota and neurological effects of glyphosate. Neurotoxicology 75, 1–8. https://doi.org/10.1016/j.neuro.2019.08.006.

Russo, I., Gavello, D., Menna, E., Vandael, D., Veglia, C., Morello, N., Corradini, I., Focchi, E., Alfieri, A., Angelini, C., Bianchi, F.T., Morellato, A., Marcantoni, A., Sassoè-Pognetto, M., Ottaviani, M.M., Yekhlef, L., Giustetto, M., Taverna, S., Carabelli, V., Matteoli, M., Carbone, E., Turco, E., Defilippi, P., 2019. p140Cap regulates GABAergic synaptogenesis and development of hippocampal inhibitory circuits. Cerebr. Cortex 29, 91–105. https://doi.org/10.1093/cercor/bhx306.

Schneggenburger, R., Meyer, A.C., Neher, E., 1999. Released fraction and total size of a pool of immediately available transmitter quanta at a calyx synapse. Neuron 23, 399–409. https://doi.org/10.1016/s0896-6273(00)80789-8.

Schönbrunn, E., Eschenburg, S., Shuttleworth, W.A., Schloss, J.V., Amrhein, N., Evans, J. N., Kabsch, W., 2001. Interaction of the herbicide glyphosate with its target enzyme 5-enolpyruvylshikimate 3-phosphate synthase in atomic detail. Proc. Natl. Acad. Sci. U. S. A. 98, 1376–1380. https://doi.org/10.1073/pnas.98.4.1376.

Shende, V.V., Bauman, K.D., Moore, B.S., 2024. The shikimate pathway: gateway to metabolic diversity. Nat. Prod. Rep. 41, 604–648. https://doi.org/10.1039/d3np00037k.

Silver, R.A., Momiyama, A., Cull-Candy, S.G., 1998. Locus of frequency-dependent depression identified with multiple-probability fluctuation analysis at rat climbing fibre-Purkinje cell synapses. J. Physiol. 510 (Pt 3), 881–902. https://doi.org/10.1111/j.1469-7793.1998.881bj.x.

Tang, X., Jaenisch, R., Sur, M., 2021. The role of GABAergic signalling in neurodevelopmental disorders. Nat. Rev. Neurosci. 22, 290–307. https://doi.org/10.1038/s41583-021-00443-x.

Traynelis, S.F., Jaramillo, F., 1998. Getting the most out of noise in the central nervous system. Trends Neurosci. 21, 137–145. https://doi.org/10.1016/s0166-2236(98)01238-7.

Zhao, H., Mao, X., Zhu, C., Zou, X., Peng, F., Yang, W., Li, B., Li, G., Ge, T., Cui, R., 2021. GABAergic system dysfunction in autism spectrum disorders. Front. Cell Dev. Biol. 9, 781327. https://doi.org/10.3389/fcell.2021.781327.